Available online at www.sciencedirect.com
SCIENCE DIRECT®
Journal of Solid State Chemistry 171 (2003) 143–151
JOURNAL OF SOLID STATE CHEMISTRY
http://elsevier.com/locate/jssc

Ternary and higher order rare-earth nitride materials: synthesis and characterization of ionic-covalent oxynitride powders

Franck Tessier and Roger Marchand*

Laboratoire "Verres et Céramiques" (UMR CNRS 6512), Institut de Chimie de Rennes, Université de Rennes 1, Campus de Beaulieu, F-35042 Rennes cedex, France

Received 22 May 2002; received in revised form 1 September 2002; accepted 17 November 2002

Abstract

The possibility to introduce nitrogen as a substitute for oxygen within the anionic network of ternary and higher order rare-earth oxides has been examined. The higher anionic formal charge resulting from this N^{3-}/O^{2-} substitution can be compensated either through cross-substitutions or by the creation of anionic vacancies. Resulting oxynitrides belong to different structures types which are well known in the oxide crystal chemistry. A commonly used synthesis method consists of a thermal nitridation in flowing ammonia of corresponding rare-earth oxide compositions. In such a solid–gas process the reactivity of the oxide precursors is an important reaction parameter, and a soft chemistry route involving a complexing method may be advantageously utilized to prepare them. The N^{3-}/O^{2-} anionic substitution induces also a more covalent character illustrated, for example, by strongly colored oxynitride powders that gives the possibility to tune the absorption edge of the UV–visible spectra by suitable adjustment of the N/O ratio.

Keywords: Rare earth; Transition metal; Oxynitride; Ammonolysis; Crystal chemistry; Color

1. Introduction

The combination of nitrogen with less electronegative elements results in nitrides, corresponding to a trivalent state of nitrogen with a -3 more or less formal charge. However, in relation with the large triple bond energy in dinitrogen—941 kJ mol^{-1}—compared to oxygen—499 kJ mol^{-1}— nitrides are much less numerous than oxides. A direct combination with nitrogen generally requires elevated temperatures and implies total absence of oxygen to prevent either a preferential reaction or that comes to the same thing, an attack of the nitride as

$$\text{nitride} + O_2 \xrightarrow{T} \text{oxide} + N_2^{\uparrow}.$$

Thus, nitrogen (Pauling's electronegativity = 3.0) forms with rare-earth metals *R*, whose electronegativities range from 1.1 to 1.3, stable *R*N mononitrides characterized in particular by high melting points, around 2500°C, and at least formally, involving the trivalent oxidation state of the metal atom. The large difference in electronegativity explains the predominant ionic character—more than 50%—of the *R*–N bond that results in binary nitrides highly sensitive to hydrolysis.

This paper is devoted to multinary rare-earth nitride materials [1], i.e., to compounds in which other cationic/anionic elements are associated with rare-earth metals and nitrogen. More precisely, it will focus on *R*–*M*–O–N quaternary oxynitride systems, where *M* is a transition metal, and will be limited in principle to purely ionic-covalent compounds, i.e., with the metal *M* in its highest oxidation state.

With regard to the *R*N binary nitrides, two main differences may be pointed out, the one concerns the behavior in ambient air, the other one the synthesis conditions. On one hand, quaternary *R*–*M*–O–N oxynitrides, like *R*–*M*–O oxides, do not show any hygroscopic character that makes it possible to exploit characteristic features. On the other hand, whereas the rare-earth binary oxides have a large negative free energy of formation that explains they do not react with ammonia, a very common synthetic route to *R*–*M*–O–N oxynitrides consists of the reaction of a corresponding

*Corresponding author. Fax: +33-2-2323-5683.
E-mail address: roger.marchand@univ-rennesl.fr (R. Marchand).

0022-4596/03/$ - see front matter © 2003 Elsevier Science (USA). All rights reserved.
doi:10.1016/S0022-4596(02)00201-3

R–*M*–O ternary oxide with flowing ammonia at temperatures generally ranging between 700°C and 1000°C. This reaction is therefore able to create *R*–N bonds from *R*–O bonds, in accordance with the general equation:

$$R_aMO_x + zNH_3 \rightarrow R_aMO_yN_z + (x-y)H_2O^{\uparrow}$$

with $z = 2/3(x-y)$ if one considers that the oxidation state of *M* (and of *R*) remains unchanged. An interesting fact to be noticed is precisely this possibility to maintain the highest oxidation state of the transition metal, for example Ti^{+IV} or W^{+VI}, although the corresponding binary nitrides are unknown, and despite reducing ammonia synthesis conditions [2]. This can be attributed to the electropositive character of rare-earth cations through an inductive effect [3], and maybe also to a stabilizing effect of the lattice energy of the $R_aMO_yN_z$ crystal structure.

In such oxynitrides, nitrogen and oxygen, generally speaking, play a similar role within the anionic subnetwork, so that they may be regarded from a crystal chemistry point of view as pseudo-oxides, i.e., as oxides in which part of oxygen has simply been replaced by nitrogen. So, they may belong to structure types which are well known in oxide crystal chemistry, and moreover, their properties may be easily compared with those of parent oxides.

Trivalent nitrogen anions, N^{3-}, substituting for divalent oxygen anions, O^{2-}, induce an increase in the anionic formal charge which can be compensated according to two different principles. In the first case, a cross-substitution principle is applied which allows the same stoichiometry to be kept, and very possibly, the same structure, provided size conditions are obeyed. In other words, trivalent rare-earth elements which form strong bonds with nitrogen are ideal substitutes to ensure the charge balance by replacing divalent alkaline-earth or monovalent alkali cations, for instance, according to

$$R^{3+} + N^{3-} = Ca^{2+} + O^{2-},$$

$$R^{3+} + 2N^{3-} = Na^{+} + 2O^{2-}.$$

This is illustrated by *R*–*M*–O–N oxynitrides with scheelite-, pyrochlore-, perovskite- and fluorite-type structures. In the second case, the anionic charge compensation is carried out in rare-earth ternary or higher order oxides, according to $2N^{3-}$ replacing $3O^{2-}$. A particularly favorable situation is encountered when the crystal structure has enough flexibility to accept the consequent anion deficiency, as is illustrated by rare earth and tungsten oxynitrides with a fluorite-related structure, for which the following equation may be written:

$$2N^{3-} + 1\square = 3O^{2-}.$$

As nitrogen is less electronegative than oxygen—3 versus 3.5 in the Pauling's scale—another consequence of the N/O substitution is an increase in the covalent character which results in significant modifications in chemical and physical properties. A typical feature is the color of the *R*–*M*–O–N oxynitride powders [4].

2. Experimental

It is well known that the syntheses of nitrides or oxynitrides do not follow well-established rules. The main problem is that there exists no ammonolysis systematics: each system represents a particular case and is likely to react differently as a function of several intrinsic (reacting components) or extrinsic (temperature, reaction time, furnace atmosphere, …) parameters. Solid/gas reactions are the most usual routes to oxynitrides. Nitridation reactions are generally carried out in an alumina boat containing the oxide precursor powder placed inside an alumina tube through which ammonia gas flows generally at a rate up to 30–40 $l\,h^{-1}$ at 800°C. The temperature is raised in the range 600–1000°C, depending on the precursor and system used, with a heating rate of about 10°C min^{-1}. Ammonia acts as both a reducing and a nitriding (oxidizing) agent. The ammonia flow rate depends on the reaction temperature: the higher the temperature, the higher the rate, in order to minimize the dissociation of NH_3 into dinitrogen and dihydrogen before reaching the product. According to the reaction temperature and the nature of the used oxide precursor, a reducing character may predominate or not. This dual behavior—nitriding and reducing—is essential for the ammonolysis reaction. Indeed, while nitrogen is incorporated, hydrogen combines with oxygen atoms from the oxide and eliminates them as water vapor:

$$\text{oxide} + NH_3(g) \rightarrow \text{oxynitride} + H_2O^{\uparrow}(g).$$

Typically after reaction, the furnace is switched off and the powder is allowed to cool to room temperature under a nitrogen atmosphere.

The success of the solid/gas ammonolysis depends highly on the nature of the precursors. The preparation of ammonolysis precursors by solid state methods has shown limits regarding their homogeneity and reactivity. Pure single phases are often difficult to prepare: as an example, 5–6 heating steps at 1300°C during 20 h each are necessary to obtain pure tungstates R_6WO_{12} from binary oxides. The difficulty increases with multinary cationic stoichiometries, due to the numerous compositions potentially accessible. The specific surface areas of the powders are generally small, around a few $m^2\,g^{-1}$, inducing low reactivity. High temperatures may also cause loss of one of the components, such as WO_3 which sublimes at 800°C. So, to obtain R_6WO_{12} powders, a

first heating step between 700°C and 800°C is necessary to combine WO_3 and R_2O_3, so that intermediate by-products need then to be dissociated to reach the desired stoichiometry $R/W = 6$.

Numerous *chimie douce*-type processes have been developed to prepare oxide powders in order to improve their quality (purity, chemical homogeneity, etc.) and their reactivity. For example, the "Pechini" and the "amorphous citrate" routes have been often used to synthesize several oxynitride compounds mentioned in this paper. This process utilizes citric acid as a complexing agent and is not, strictly speaking, a classic sol–gel process in the usual sense that the gel is not formed by a metal–oxygen–metal network, but rather from a calcination of metal–organic complexes, thus producing ultrafine reactive powders with a good chemical homogeneity. The citrate route can be generalized to synthesize a large number of compositions which cannot be obtained via traditional methods. The use of citric acid presents several advantages such as formation of very stable solutions of more or less complex stoichiometries. The cation stoichiometry being the same in the solution and in the powdered residue after calcination, all designed powder compositions may be easily and rapidly synthesized by this aqueous process. Thus, complexation–calcination-type methods, and particularly the citrate route, constitute a suitable answer to the above-mentioned problematics. The experimental route to the tungstates R_6WO_{12} is described in the flowchart drawn in Fig. 1. Similar experimental methods are also proposed in other papers [5–7].

3. Crystal chemistry of cross-substituted $R-M-O-N$ oxynitrides

Association of a rare-earth element and a transition metal within *R*–*M*–O–N quaternary oxynitride compositions gives rise to a wide array of structure types. The differences between the size of rare-earth and transition elements explain, for a large part, the resulting structures. Three types of coordination polyhedra—tetrahedral, octahedral and cubic—characterize the environment of *M* cations. The larger rare-earth atoms occupy holes formed by the different arrangements of these structural units. Typical features and recent results

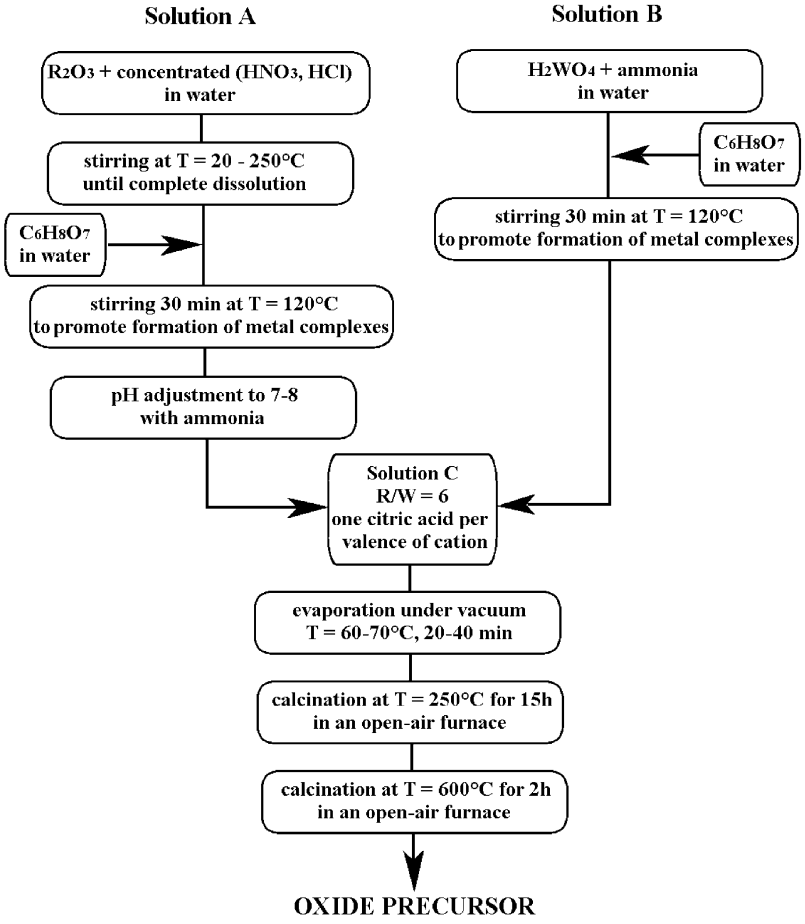

Fig. 1. Flowchart for preparing R_6WO_{12} tungstates by the amorphous citrate method.

are described below in scheelite, pyrochlore, perovskite and fluorite structures.

3.1. Scheelite-type structure

The following cross-substitution in the scheelite representative term $CaWO_4$:

$$R^{3+}+N^{3-}=Ca^{2+}+O^{2-}$$

leads to an isostructural oxynitride series RWO_3N with R = Nd, Sm, Gd or Dy. These compounds are prepared by solid–gas reaction between corresponding tungstates $R_2W_2O_9$ and flowing ammonia at 700–750°C. Their tetragonal ($I4_1/a$) structure is comprised of isolated [WO_3N] tetrahedra linked to each other by R cations, the coordination number of which is 8. Table 1 compares the unit cell parameters of $CaWO_4$ with those of the oxynitride phases. These compounds present an insulating behavior totally coherent with tungsten being at its highest oxidation state +VI, which is thus stabilized in a tetrahedral nitrogen-containing environment. However, two facts were a priori unfavorable to keep this high oxidation state: the reducing character of ammonia and the fact that no corresponding nitride (WN_2) exists in the W–N binary system, where only W_2N and WN are known.

As previously mentioned [8], neodynium marks a transition in the lanthanide series since simultaneous formation of both a scheelite phase and a nitrogen-rich perovskite-type phase $NdW(O,N)_3$ is observed in that case. A competition exists between formation of scheelite and perovskite, the latter being favored by a higher temperature and longer reaction times. Air stable $SmWO_3N$ and $GdWO_3N$ have been isolated as single phases. $Eu_2W_2O_9$ reacts with ammonia without producing a similar oxynitride phase, although $r_{Sm^{3+}} < r_{Eu^{3+}} < r_{Gd^{3+}}$ (r: ionic radius). This result evidences a reduction of trivalent europium under the experimental conditions. For ions smaller than gadolinium, no corresponding ternary oxide exists with the ratio $R/M = 1$. A thermal treatment in air, followed by nitridation, of a mixture Dy_2O_3–$2WO_3$ leads to a partially formed $DyWO_3N$ phase.

A light gray-colored $NdWO_3N$ sample has been recently isolated as a single phase by nitriding, at a temperature as low as 600°C, a more reactive $Nd_2W_2O_9$ precursor obtained via the amorphous citrate process (the reaction onset of a "classic" ternary oxide is 700°C). So, an improved precursor reactivity makes possible an extension of the stability domain of the scheelite. By using the same precursor synthesis method, solid solutions have been envisaged between $M^{+II}WO_4$ and RWO_3N (M^{+II} = alkaline earth) whose preparation and characterizations are now in progress [9].

Table 1
Unit cell parameters of scheelite-type RWO_3N oxynitrides (R = Nd, Sm, Gd, Dy)

RWO_3N	a (Å)	c (Å)	V (Å^3)
R = Nd	5.287(5)	11.57(1)	323
Sm	5.248(2)	11.46(1)	316
Gd	5.225(2)	11.34(1)	310
Dy	5.189(3)	11.32(1)	305
$CaWO_4$	5.243	11.376	313

3.2. Pyrochlore-type structure

$RTaO_4$ (R = Nd → Yb, Y) precursors react with NH_3 at 900–950°C to form pyrochlore-type $R_2Ta_2O_5N_2$ oxynitrides [10]. In the case of lanthanum, only a perovskite-type phase $LaTaON_2$ was identified. From neodynium to dysprosium, along with a decrease in the rare-earth ionic radius, the pyrochlore structure coexists with a nitrogen-rich perovskite-type phase. The stability of the pyrochlore structure increases with smaller R^{3+} radii, so that single phase $R_2Ta_2O_5N_2$ (R = Er → Yb, Y) pyrochlores were easily isolated.

From a crystallographic viewpoint, the general formula may be written $A_2B_2X_6X'$, the variable value of the coordinate x of the anions X being responsible for the more or less distorted environment of the cations A ($6X+2X'$) and B ($6X$). In $R_2Ta_2O_5N_2$ oxynitrides, the distorsion is expected to be maximum for the largest rare-earth elements, the trigonal antiprism around tantalum atoms (B) thus becoming an octahedron, whereas the R elements having a smaller ionic radius would tend towards a defect fluorite structure. Cubic pyrochlore-type (space group $Fd3m$) lattice parameters have been listed from 10.56 Å for R = Nd to 10.235 Å for R = Yb [10]. We have recently revisited this series of oxynitrides described previously as pyrochlores. While the pyrochlore structure was confirmed for the larger rare earths (Nd or Sm) due to the clear presence of low intensity X-ray diffraction peaks, a fine study of smaller R-containing phases (R = Dy → Yb, Y) reveals something different. Actually, in the absence of additional weak peaks, the X-ray powder patterns can be indexed in a defect fluorite-type unit cell with 1/8 the volume (space group $Fm\bar{3}m$) [11].

As illustrated in the case of rare-earth hafnates $R_2Hf_2O_7$ [12], two main criteria explain the structural ordering: one is the large charge difference between two ions, the other is their size difference. When the size difference is significant, ordering occurs. For the smaller rare earths, this difference is diminished and ordering may disappear. From neutron diffraction data, we have indexed $Y_2Ta_2(O,N,\square)_8$ in a defect fluorite-type unit cell ($a = 5.153$ Å), implying both an anionic and a cationic disorder.

A molybdenum oxynitride pyrochlore $Sm_2Mo_2O_{3.83}N_{3.17}$ ($a = 10.4975(5)$ Å) has been synthesized by

heating the oxide pyrochlore $Sm_2Mo_2O_7$ under NH_3 flow at 625°C [13]. The significantly larger than 4+ formal oxidation state of Mo (~5.6+) shows the preponderant oxidizing (nitriding) role of NH_3 in that case over its generally more reducing character.

Note also that Dolgikh and Lavut [14] have reported the preparation of Ti^{+IV} oxynitride pyrochlore phases $R_2Ti_2O_{5.5}N$ (R=Sm, Dy, Y) when reacting oxide pyrochlores $R_2Ti_2O_7$ with ammonia at 1000°C.

3.3. Perovskite-type structure

Conditions to form oxynitride perovskites have been previously reported [1,15]. Note that all the $RMO_{3-x}N_x$ compositions can be derived from the well-known compound $BaTiO_3$ by cross-substitutions. Perovskite-type oxynitrides $RTiO_2N$ (R=La, Nd), $RTaON_2$ (R=La–Dy) and $LaNbON_2$ were prepared at 950°C from the corresponding ternary oxide heated in flowing ammonia, and characterized as orthorhombic $GdFeO_3$-type perovskites [16].

$LaTiO_2N$ and $NdTiO_2N$, in which the titanium +IV oxidation state is stabilized, crystallize almost with the same unit cell as the $RTiO_3$ oxide perovskites which formally correspond to Ti^{+III}. But, $LaTiO_2N$ and $NdTiO_2N$ present an insulating behavior, whereas $LaTiO_3$ is metallic at $T>-170$°C, $NdTiO_3$ is a semiconductor at room temperature [17,18] and $Nd_{1-x}TiO_3$ phases show remarkable changes in properties with vacancy "doping" on the R site [19].

Several structures of oxynitrides have been re-examined using neutron diffraction. As X-ray diffraction does not allow oxygen and nitrogen to be distinguished because of very close values of their atomic scattering factors, neutron diffraction is an ideal method to study oxynitrides because the scattering lengths of these two elements—$b(O)=0.58\times10^{-12}$ cm, $b(N)=0.94\times10^{-12}$ cm—are sufficiently different to permit detection of structural order between oxygen and nitrogen atoms, the latter being in addition the strongest scatterer in the structure. A recent neutron diffraction study [20] confirmed the $GdFeO_3$-distorted perovskite structure of $NdTiO_2N$ (*Pnma*, $a=5.5492(1)$ Å, $b=7.8017(1)$ Å, $c=5.52901(9)$ Å). However, a different unit cell of triclinic symmetry was found for $LaTiO_2N$ ($I\bar{1}$, $a=5.6097(1)$ Å, $b=7.8719(2)$ Å, $c=5.5752(1)$ Å, $\alpha=90.199(2)°$, $\beta=90.154(3)°$, $\gamma=89.988(8)°$), thus evidencing two kinds of $Ti(O_4N_2)$ octahedra, but without any O/N ordering. An oxynitride perovskite $LaZrO_2N$ (*Pnma*, $a=5.87525(5)$ Å, $b=8.25031(7)$ Å, $c=5.81008(5)$ Å) was also obtained by reacting under NH_3 flow an X-ray amorphous $La_2Zr_2O_7$ precursor prepared via the citrate route. In none of these three phases was oxygen/nitrogen order found [20].

Due to their insulating properties, the $RTiO_2N$, $RTaON_2$ and $LaNbON_2$ oxynitrides as well as $BaTaO_2N$ and $BaNbO_2N$, have been considered as possible substitutes for $BaTiO_3$-based materials for high dielectric constant ceramic capacitors [21]. Oxynitride thin films $LaNb(O_yN_2)_x$ were prepared by reactive sputtering under $Ar+N_2$ atmosphere from a multiphase LaN+NbN target [22].

The crystal structure of $LaTaON_2$ has been recently revisited using neutron diffraction. $LaTaON_2$ crystallizes monoclinic ($C2/m$, $a=8.0922(3)$ Å, $b=8.0603(2)$ Å, $c=5.7118(2)$ Å, $\beta=134.815(1)°$) and presents a totally ordered oxygen/nitrogen anionic network shown in Fig. 2 [23], with oxygen atoms located in the median plane of TaO_2N_4 octahedra.

The alkali metal and tantalum oxynitride perovskites $A_xLa_{2/3}Ta_2O_{6-x}N_x$ (A=Li, Na) were studied with respect to ionic conductivity [24]. They were synthesized by reacting $La_{2/3}Ta_2O_6$ with Li(OH) or $NaNO_3$, respectively, at 600–950°C in NH_3 gas atmosphere. All these phases are of the $La_{2/3}Ta_2O_6$ structure type ($P4/mmm$, $a\sim3.92$ Å, $c\sim7.91$ Å) and correspond therefore to an alkali metal ion intercalation compensated by a parallel N/O substitution. In the same work [24], $Li_2LaTa_2O_6N$ was isolated in the reaction of Li_2CO_3, $La(OH)_3$, and Ta_2O_5 under ammonia at 800–900°C. This new oxynitride belongs to the Ruddlesden–Popper family of $Sr_{n+1}Ti_nO_{3n+1}$ with $n=2$ perovskite-like phases ($I4/mmm$, $a=3.9506(5)$ Å, $c=18.456(6)$ Å).

Considering now $BaTiO_3$ and the double cross-substitution W^{+VI}/Ti^{+IV} and R^{3+}/Ba^{2+}, pure nitride perovskite compositions RWN_3 were expected to form.

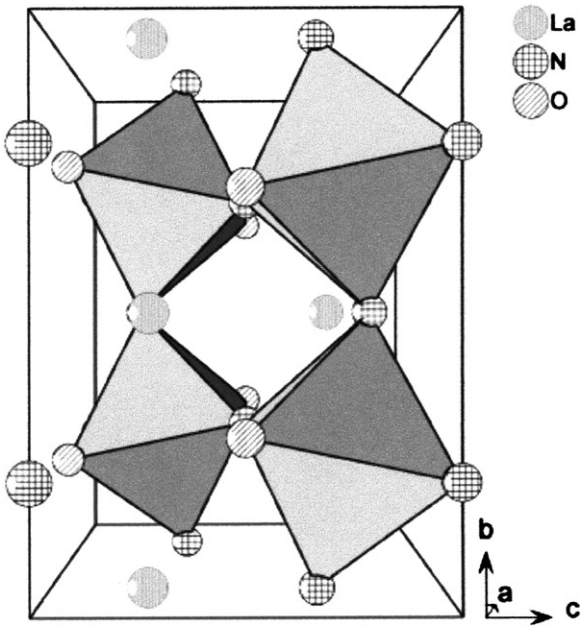

Fig. 2. Oxygen/nitrogen ordering within the $LaTaON_2$ unit cell (after [23]).

However, thermal ammonolysis of the tungstates $R_2W_2O_9$ (700–900°C) leads to mixed-valence conducting oxynitride perovskites RWO_xN_{3-x} in which W does not maintain its maximum oxidation state [25]. The X-ray diffraction cubic unit cell parameters range from $a = 3.994$ Å (R = La) to 3.964 Å (R = Nd). A time-of-flight neutron diffraction study, performed on $LaWO_{0.6}N_{2.4}$ reveals a tetragonal unit cell ($I\bar{4}$, $a = 5.6523(6)$ Å, $c = 8.0084(15)$ Å, $c/a = 1.4168$) with disordered O and N atoms. Fig. 3 displays that the $W(O,N)_6$ octahedra are slightly turned along the c-axis. The RWO_xN_{3-x} perovskites (R = La, Nd) adopt an n-type semiconducting behavior [26]. In the La–V–O–N system, the perovskite-type homogeneity domain ranges from $LaVO_3$ to $LaVO_{2.1}N_{0.9}$ with vanadium at the V^{+III}–V^{+IV} mixed-valent state in the $LaVO_{3-x}N_x$ oxynitride perovskites which behave as p-type semiconductors [27].

The K_2NiF_4-type structure which is closely related to the perovskite structure is exhibited by the oxynitride Nd_2AlO_3N (Fig. 4) another typical example of oxygen/nitrogen order [28]. However, no analogous phase containing both a rare-earth element and a transition metal has been indexed to date within this structure type. The two possible stoichiometries would be $R_2MO_2N_2$ or R_2MON_3.

3.4. Fluorite-type structure

The thermal nitridation in flowing ammonia of different rare-earth tungstates leads to fluorite-type oxynitrides $(R,W)_4(O,N,\square)_8$ in which the highest oxidation state of tungsten is kept. Among the numerous R–W–O possible starting oxide compositions, the three following precursors, R_2WO_6 ($R/W = 2$), $R_{14}W_4O_{33}$ ($R/W = 3.5$) and R_6WO_{12} ($R/W = 6$) were particularly studied [29]. From R_2WO_6, brown-colored oxynitride powders were prepared with the general composition $A_4X_{6.6}$ ($A = \Sigma$ cations, $X = \Sigma$ anions), about halfway between the CaF_2 (A_4X_8) fluorite and Mn_2O_3 (A_4X_6) bixbyite stoichiometries (Fig. 5). These anion-defect fluorite-type phases crystallize in a cubic unit cell ($Fm\bar{3}m$) with a unit cell parameter ranging from $a = 5.383(1)$ Å for R = Nd to $a = 5.164(2)$ Å for R = Yb. This means that both anionic and cationic subnetworks are disordered. In particular, it is necessary that R and W atoms occupy the same 4a position in spite of quite different ionic radii. A neutron diffraction study undertaken on the composition $Y_{2.67}W_{1.33}O_{3.8}N_{2.8}\square_{1.4}$ suggests, however, a more complex solution, as indicated by a too high

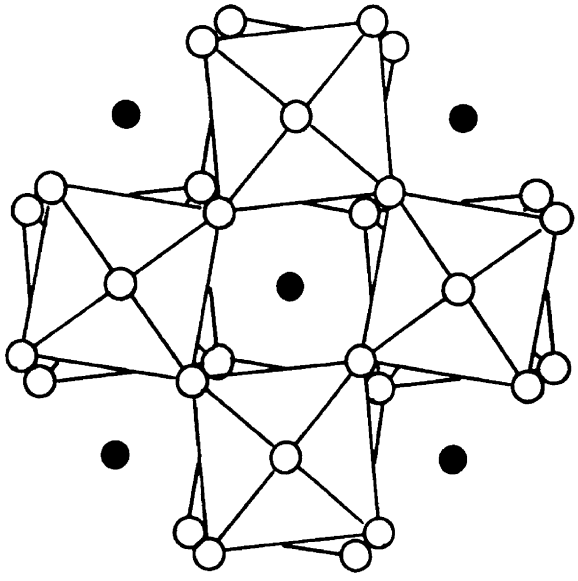

Fig. 3. Projection onto the (001) plane of the tetragonal structure of $LaWO_{0.6}N_{2.4}$ evidencing a $\pm 8°$ rotation of $W(O,N)_6$ octahedra. Open circles represent anions (O, N) and solid circles are La atoms. W atoms are not drawn.

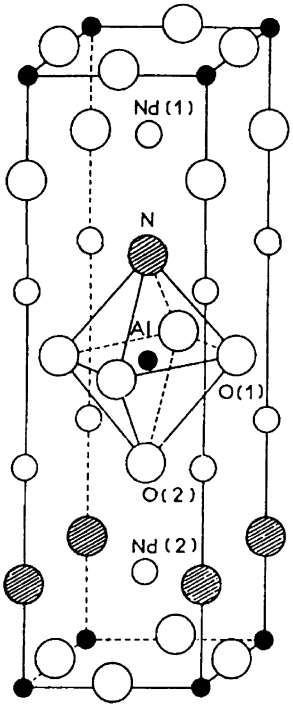

Fig. 4. Crystal structure of Nd_2AlO_3N ($I4mm$). O(1) atoms are at bridge sites, O(2) and N are at apical sites.

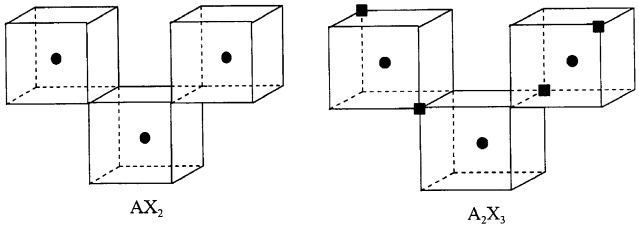

Fig. 5. Structural filiation between fluorite CaF_2 (A_4X_8) and bixbyite Mn_2O_3 ($A_4X_6\square_2$).

experimental value of the anion isotropic displacement parameter [29].

Starting from the anion-defect fluorite-type oxides $R_{14}W_4O_{33}$ and R_6WO_{12}, a progressive substitution of nitrogen for oxygen was observed with the formation of two solid solution domains, as described in more details in the following section. In the same way, ammonolysis of $Gd_{14}W_4O_{33}$ at 700–1000°C yielded an oxynitride series $Gd_{14}W_4O_{33-x}N_y$ with $0 \leqslant x \leqslant 17 \pm 2$ and $0 \leqslant y \leqslant 9 \pm 2$ [30]. A first indexation in a body-centered monoclinic unit cell deriving from that of fluorite was revised by neutron diffraction, indicating a considerably larger unit cell.

4. Optical absorption properties: effects of a progressive N/O substitution

The transformation by thermal ammonolysis of rare-earth and transition metal oxides into oxynitrides, i.e., the introduction within the anionic subnetwork of a less electronegative element than oxygen, induces a more covalent character which can give rise to strongly colored powders.

The color is determined by the position of the absorption edge of the diffuse reflectance spectrum. For white-colored oxide powders (for example, Li_2O, MgO, Ta_2O_5, etc.), the absorption edge is located within the UV part of the electromagnetic spectrum, while it is known to be shifted into the visible part of the spectrum for corresponding nitride compounds: Li_3N is red–brown [31,32], Mg_3N_2 yellow [33–35], Ta_3N_5 red–orange [36–41], TaON yellow [42].

In the ionic-covalent semiconducting compounds considered here, the color originates from electronic interband transitions between the occupied valence band and the vacant conduction band. An increased covalent character induces a decrease in the width of the optical band gap and in a possible selective absorption of visible light. This is shown by the color of several above-described *R*–*M*–O–N quaternary oxynitrides. Whereas $BaTiO_3$ is white, $LaTiO_2N$ is brown, $LaTaON_2$ is red–brown, $GdTaON_2$ is yellow [43], and intermediate colors can also be obtained with solid solutions, for example between red–brown and yellow in the $La_{1-x}Ca_xTaO_{1+x}N_{2-x}$ $(0<x<1)$ solid solution [44]. However, the ideal situation to demonstrate existence of a close relationship between the shift of the absorption edge towards higher wavelength values and the presence of nitrogen is to compare totally analogous oxide and nitrided powders, i.e., not only having the same general anion/cation stoichiometry and belonging to the same structure type, but involving in addition the same cations. As the electroneutrality rule requires that $3O^{2-}$ are replaced by $2N^{3-}$, this case can only be encountered with structures, such as the fluorite structure, able to show enough flexibility to accept anionic vacancies, according to the following equation:

$$3O^{2-} = 2N^{3-} + 1\square$$

with one vacancy created per two introduced nitrogen atoms.

This concept is illustrated in particular by the rare-earth tungstates R_6WO_{12} and $R_{14}W_4O_{33}$ mentioned above whose crystal structure is already by itself an anion-defect fluorite structure, as shown by their respective formulas $(R_{3.43}W_{0.57})(O_{6.85}\square_{1.15})$ and $(R_{3.11}W_{0.89})(O_{7.33}\square_{0.67})$, expressed respecting a A_4X_8 general fluorite-type formulation ($A = \Sigma$ cations, $X = \Sigma$ anions). Their nitridation is written as

$$R_6WO_{12}\square_2 + 2xNH_3 \rightarrow R_6WO_{12-3x}N_{2x}\square_{2+x} + 3xH_2O^{\uparrow},$$

$$R_{14}W_4O_{33}\square_3 + 2xNH_3 \rightarrow R_{14}W_4O_{33-3x}N_{2x}\square_{3+y} + 3xH_2O^{\uparrow}.$$

The amount of incorporated nitrogen progressively increases as a function of nitridation temperature and time, thus delimiting in each case a large oxynitride solid solution domain. The compositions range from $R_{3.43}W_{0.57}O_{6.85}\square_{1.15}$ to $R_{3.43}W_{0.57}O_{4.3}N_{1.7}\square_2$ for $R/W = 6$, and from $R_{3.11}W_{0.89}O_{7.33}\square_{0.67}$ to $R_{3.43}W_{0.89}O_{3.4}N_{2.6}\square_2$ for $R/W = 3.5$ (Fig. 6). So, in both cases the maximum nitrogen content reached corresponds to the same maximum amount of vacancies (2 out of 8 anions), in other words to the same minimum anion/cation ratio $(O+N)/(R+W) = 1.5$.

This $A_4B_6\square_2$ stoichiometry is that of the bixbyite whose structure is an anion-defect fluorite structure with

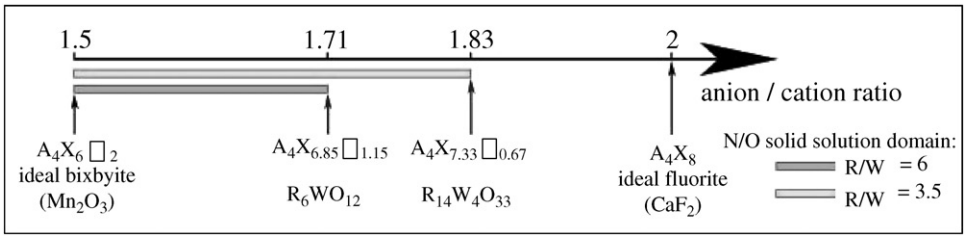

Fig. 6. N/O solid solution domains $R_{14}W_4O_{33-3x}N_{2x}$ and $R_6WO_{12-3x}N_{2x}$ resulting from thermal ammonolysis of the corresponding oxides $R_{14}W_4O_{33}$ and R_6WO_{12}.

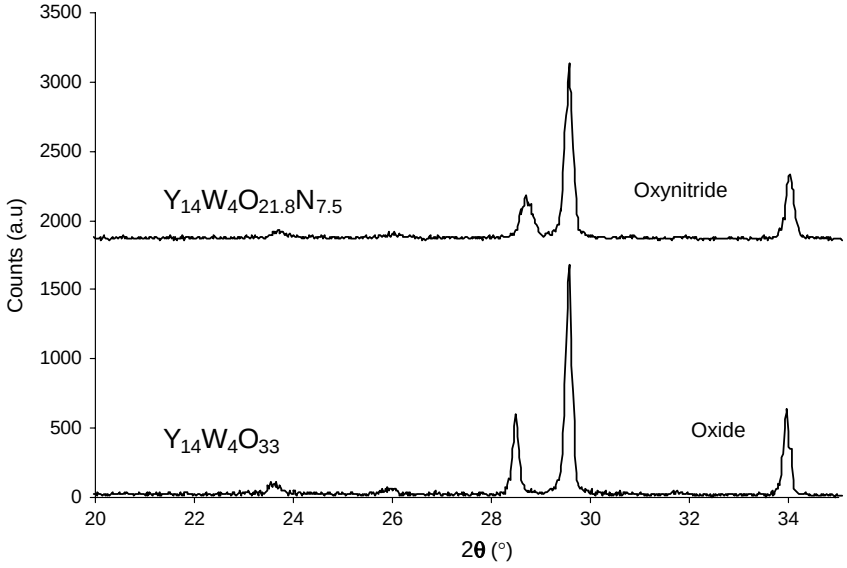

Fig. 7. Compared X-ray diffraction powder patterns of fluorite-type Y/W/O oxide and Y–W–O–N oxynitride.

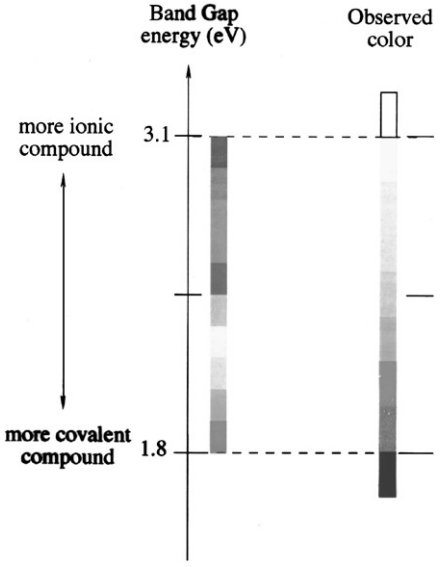

Fig. 8. Relationship between the band gap width and the observed color.

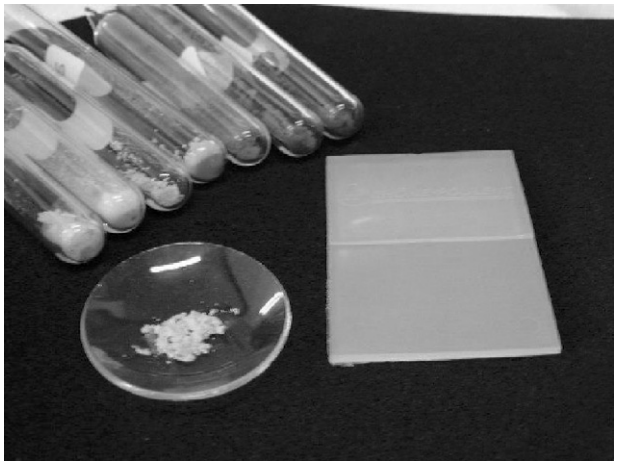

Fig. 9. A palette of colored oxynitride powders resulting from thermal ammonolysis of white oxide precursors.

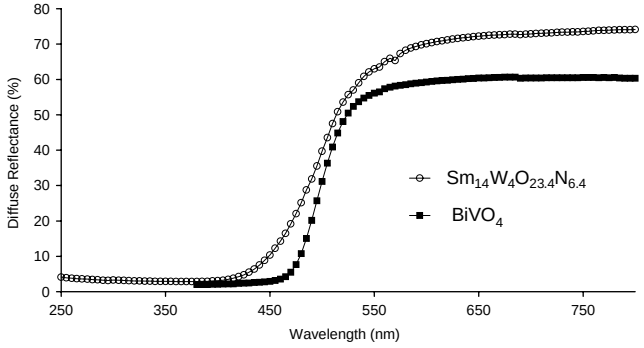

Fig. 10. Diffuse reflectance spectrum of the $Sm_{14}W_4O_{23.4}N_{6.4}\square_{6.2}$ composition compared to the industrial pigment $BiVO_4$.

two vacancies per anion cube being arranged alternatively along a cube diagonal and a side diagonal. However, as exemplified in Fig. 7, X-ray diffraction powder patterns corresponding to the two above oxynitride series only show, in a first approximation, a cubic $Fm\bar{3}m$ symmetry of a disordered fluorite type. Compared to that of the precursor oxide (Fig. 7), the X-ray powder pattern of the nitrided composition only shows an enlargement and a slight shift of the diffraction peaks.

As the only variable of the solid solution domain is the nitrogen content, it is possible to observe a continuous variation of the absorption edge position, and therefore of the color, only as a function of progressive nitrogen enrichment. This color means a progressive decrease in the band gap energy value corresponding itself to a progressively more covalent character. Starting from a white-colored powder, i.e.,

absorbing in UV, when the gap becomes lower than 3.1 eV, a part absorption takes place and the powder becomes colored from pale yellow to yellow, orange, red, as displayed in Fig. 8.

Some of these oxynitride compositions have potential as new inorganic pigments in paints and plastics as substitutes for heavy metals-based toxic pigments (Fig. 9). Fig. 10 shows an example of a yellow oxynitride powder compared to a commercial pigment. Note that an important characteristic for a given color is of course the position of the absorption edge which can be tuned at a precise value versus nitrogen content, and also its stiffness which is responsible of the color purity.

References

[1] R. Marchand, in: K.A. Gschneider, L. Eyring (Eds.), Handbook on the Physics and Chemistry of Rare Earths, Vol. 25, Elsevier, 1998, pp. 51–100 (Chapter 166).
[2] R. Marchand, F. Tessier, A. Le Sauze, N. Diot, Int. J. Inorg. Mater. 3 (2001) 1143–1146.
[3] J. Etourneau, J. Portier, F. Ménil, J. Alloys Compds. 188 (1992) 1–7.
[4] N. Diot, O. Larcher, R. Marchand, J.Y. Kempf, P. Macaudière, J. Alloys Compds. 323–324 (2001) 45–48.
[5] A. Douy, P. Odier, Mater. Res. Bull. 24 (1989) 1119–1126.
[6] M.M. Milanova, M. Kakihana, M. Arima, M. Yashima, M. Yoshimura, J. Alloys Compds. 242 (1996) 6–10.
[7] M. Yoshimura, J. Ma, M. Kakihana, J. Am. Ceram. Soc. 81 (1998) 2721–2724.
[8] P. Antoine, R. Marchand, Y. Laurent, Rev. Int. Hautes Temp. Réfract. 24 (1987) 43–46.
[9] F. Cheviré, F. Tessier, R. Marchand, Mater. Res. Bull. (2003) in press.
[10] F. Pors, R. Marchand, Y. Laurent, J. Solid State Chem. 107 (1993) 39–42.
[11] E. Orhan, N. Pinguet, F. Tessier, R. Marchand (2003), to be published.
[12] L.H. Brixner, Mater. Res. Bull. 19 (1984) 143–149.
[13] G.M. Veith, M. Greenblatt, M. Croft, J.B. Goodenough, Mater. Res. Bull. 36 (2001) 1521–1530.
[14] V.A. Dolgikh, E.A. Lavut, Zh. Neorg. Khim. 36 (1991) 2470; R. Russ, J. Inorg. Chem. 36 (1991) 1389–1392.
[15] R. Marchand, Y. Laurent, J. Guyader, P. L'Haridon, P. Verdier, J. Eur. Ceram. Soc. 8 (1991) 197–213.
[16] R. Marchand, F. Pors, Y. Laurent, Ann. Chim. Fr. 16 (1991) 553–560.
[17] D.A. Maclean, K. Seto, J.E. Greedan, J. Solid State Chem. 40 (1981) 241.
[18] J.E. Greedan, J. Less-Common Met. 111 (1985) 335.
[19] J.E. Greedan, G. Amow, A.S. Sefat, J. Alloys Comp. (2003), in press.
[20] S.J. Clarke, B.P. Guinot, C.W. Michie, M.J.C. Calmont, M.J. Rosseinsky, Chem. Mater. 14 (2002) 288–294.
[21] R. Marchand, Y. Laurent, Composés azotés ou oxyazotés à structure pérovskite, leur préparation et leur application à la fabrication de composants diélectriques, French Patent 84–17274, 1984.
[22] Y. Cohen, I. Riess, Mater. Sci. Eng. B 25 (1994) 197–202.
[23] E. Günther, R. Hagenmayer, M. Jansen, Z. Anorg Allg. Chem. 626 (2000) 1519–1525.
[24] S. Esmaeilzadeh, J. Grins, T. Hörlin, Mater. Sci. Forum 325–326 (2000) 11–16.
[25] P. Bacher, P. Antoine, R. Marchand, P. L'Haridon, Y. Laurent, G. Roult, J. Solid State Chem. 77 (1988) 67–71.
[26] P. Antoine, R. Marchand, Y. Laurent, C. Michel, B. Raveau, Mater. Res. Bull. 23 (1988) 953–957.
[27] P. Antoine, R. Assabaa, P. L'Haridon, R. Marchand, Y. Laurent, C. Michel, B. Raveau, Mater. Sci. Eng. B 5 (1989) 43–46.
[28] R. Marchand, R. Pastuszak, Y. Laurent, G. Roult, Rev. Chim. Miner. 19 (1982) 684–689.
[29] N. Diot, O. Larcher, R. Marchand, J.Y. Kempf, P. Macaudière, J. Alloys Compds. 323–324 (2001) 45–48.
[30] M. Nilsson, J. Grins, P. Käll, G. Svensson, J. Alloys Compds. 240 (1996) 60–69.
[31] A. Rabenau, J. Schultz, J. Less-Common Met. 50 (1976) 155.
[32] H. Schultz, K. Schwarz, Acta Crystallogr. A34 (1978) 999.
[33] J. David, Y. Laurent, J. Lang, Bull. Soc. Fr. Minéral. Cristallogr. 94 (1971) 347.
[34] D.E. Partin, D.J. Williams, M. O'Keefe, J. Solid State Chem. 132 (1997) 56–59.
[35] E. Orhan, S. Jobic, R. Brec, J.Y. Saillard, R. Marchand, J. Mater. Chem. 12 (2002) 2475.
[36] G. Brauer, J.R. Weidlein, Angew. Chem. Int. Ed. Engl. 4 (1965) 241.
[37] G. Brauer, J. Weidlein, J. Strähle, Z. Anorg. Allg. Chem. 34 (1966) 298.
[38] N. Terao, Jpn. J. Appl. Phys. 10 (2) (1971) 248.
[39] J. Strähle, Z. Anorg. Allg. Chem. 402 (1973) 47.
[40] M. Jansen, E. Guenther, H.P. Letschert, Verfahren zur Herstellung von gelben und roten Pigmenten auf der Basis von Nitriden und Oxidnitriden, German Patent 199 07 618.9, 1999.
[41] M. Jansen, H.P. Letschert, D. Speer, Method of producing tantalum (V) nitride and its use, European Patent 592876, 1993.
[42] E. Orhan, F. Tessier, R. Marchand, Solid State Sci. 4 (2002) 1071.
[43] M. Jansen, H.P. Letschert, D. Speer, Cerdec AG Keramische Farben, German Patent DE4317421, Oxonitrides of the formula LnTaON2 with enhanced brightness and a process for their production and use, 1994.
[44] M. Jansen, H.P. Letschert, Nature 6781 (2000) 980–982.